J. Synchrotron Rad. (1998). **5**, 1153–1156

Synchrotron radiation direct photo-etching of polymers and crystals for micromachining

T. Katoh* and Y. Zhang

Laboratory for Quantum Equipment Technology, Sumitomo Heavy Industries Ltd, 2-1-1 Yatocho, Tanashi, Tokyo 188, Japan. E-mail: kato_tkn@tns.shi.co.jp

(*Received 4 August 1997; accepted 21 November 1997*)

Synchrotron radiation etching of polymers and optical crystals which are transparent throughout the spectral range from visible to ultraviolet has been carried out without using any chemicals, successfully creating high-aspect-ratio microstructures for micromachining. A detailed study of the etching rates by varying the synchrotron beam current, sample temperature, beam size and aspect ratio showed that this synchrotron radiation process is essentially different from laser ablation, while an *in situ* mass spectrometric analysis of gaseous etching products showed that the dissociation mechanism involved with the synchrotron radiation processing, even with heating, is completely different from the thermal dissociation of the laser ablation.

Keywords: synchrotron radiation direct etching; micromachining; high aspect ratios; Teflon polymers; optical crystals.

1. Introduction

During the past decade, powerful pulsed lasers have been widely used to etch directly (*i.e.* without using any reaction gas) materials for the formation of microstructures – a process known as laser ablation (Srinivasan & Braren, 1989). For synchrotron radiation, however, there have been few cases of the direct photo-etching process. The first synchrotron radiation direct etching (termed 'evaporation') was carried on SiO_2 by heating the sample to 1073 K (Akazawa *et al.*, 1990). The etching rate increased significantly with the temperature rise, but was very small (less than 7×10^{-3} μm min^{-1}). We found that synchrotron radiation etching (termed 'micromachining') could be carried out for a polymer, PTFE (polytetrafluoroethylene), with a much higher rate (150 μm min^{-1}); the temperature rise also increased the etching rate (Zhang & Katoh, 1996). Since white light (*i.e.* synchrotron radiation without filtering) is used, the process has to be limited to those cases in which membrane-free masks can be applied and the processing is performed in a vacuum. To remove this obstacle from micromachining applications, we recently extended the process from using white light to using X-rays, so that X-ray lithography technology (such as using an X-ray mask and processing under He atmosphere) can be simply applied. Fig. 1 shows microgears created in PTFE by synchrotron X-ray etching. Obviously such patterns cannot be created using a membrane-free mask. Recently, we applied this process to other polymers, such as PFA, FEP and PMMA, and optical crystals, such as NaCl and LiF, for micromachining (Katoh & Zhang, 1997). In order to gain a general understanding of the synchrotron radiation direct etching process, we made further detailed studies. Our results and discussions are given in the following.

Table 1
Synchrotron radiation direct etching for micromachining.

Sample substrate	PTFE	PMMA	NaCl
Sample temperature, T_s (K)	373–473	363–343	673–773
Synchrotron radiation spectra (eV)	400–5500	900–5500	White light†
Etching rate (μm min^{-1})	60	50	17
Beam current, I (mA)‡	250	310	212–282
Maximum processing depth (μm)	1500	500	1000
Maximum aspect ratio	25	5	50

† Etching has also been carried out in the spectral range 400–5000 eV with a rate 3.7 μm min^{-1}. ‡ The given beam currents were used for measurement of the above etching rates.

2. Experimental details

Some experimental details (such as the synchrotron radiation source, beamline, sample preparation and processing) can be found in our recent publication (Katoh & Zhang, 1997). The synchrotron radiation source was our 'home-made' compact superconducting electron storage ring, AURORA (575 MeV energy), now installed in Ritsumeikan University. Its synchrotron radiation had a continuous spectrum from IR to X-ray with a critical wavelength of 1.5 nm and its routine starting beam current was about 300 mA. The photon flux per beam current on the sample surface was of the order of a few 10^{15} photons s^{-1} mA^{-1} cm^{-2}. Different metallic filters were used to select synchrotron X-rays in different wavelength ranges. A 1 μm-thick Al filter, for example, was used to select X-rays mainly in the spectral range 0.4–5 keV which peaked at about 1 keV, and their photon flux on the sample surface was calculated to be about one-fifth of that of the white light. All results were reproducible by replacing the white light with its X-rays, and no consistent differences were found except that the etching rate became smaller. The etching depth was measured with either an optical microscope or a stylus profilometer. The etching rate was given by a ratio of the depth to the irradiation time, which was usually

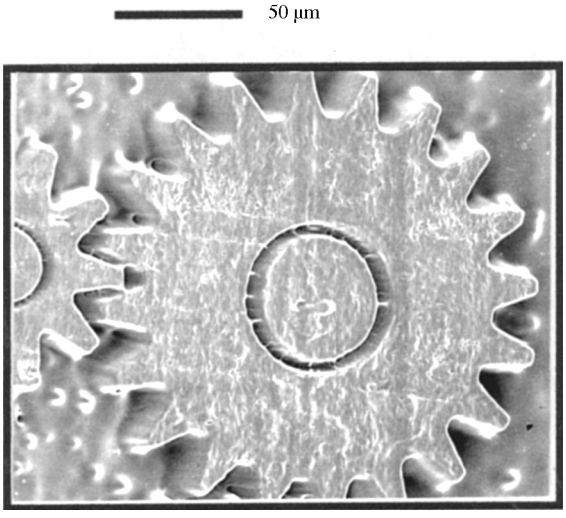

Figure 1
Scanning electron micrograph of microgears made of PTFE created by synchrotron X-ray direct etching with a proximity X-ray mask.

set to be 1 min to prevent any error due to decay of the beam current and due to the temperature rise induced by the X-irradiation. We studied the etching rate of PTFE with varying beam current (I), sample temperature (T_s), beam (or pattern) size and aspect ratio, while using the 1 μm-thick Al filter.

3. Results

Typical results are given in Table 1 and the microstructures created are shown in Figs. 1 and 2. Fig. 3 shows the etching rates (given in units of both μm min^{-1} and Å pulse^{-1}) *versus* the beam current I = 18–310 mA at T_s = RT (room temperature), 373 and 473 K in the case of PTFE. The etching rate becomes larger when the beam current (photon flux) becomes larger. The white light can give a higher etching rate due to its higher photon flux, while its X-rays can more easily be applied for the micromachining process, as mentioned above. A rise in the sample temperature results in a significant enhancement of the etching rate. With an etching rate of 60 μm min^{-1} it takes a few tens of minutes for a 1000 μm-deep processing. This means that the processing speed is much higher than that of the hard X-ray deep lithography used in the LIGA process, which usually takes a few hours or otherwise requires a synchrotron radiation source with a higher electron energy (>2 GeV) (Guckel, 1996). The processing depth has reached as high as 1500 μm in the case of PTFE. The etching rate becomes slightly higher when the beam (pattern) size for the same substrate temperature is increased.

With the minimum pattern feature of the order of a few micrometres, the quality of the microstructures which we achieved using the synchrotron radiation direct etching in PTFE and NaCl was very close to that obtained using the LIGA process in PMMA (Zhang & Katoh, 1996). For PMMA (see Fig. 2*a*), however, some thermal damage induced during the synchrotron radiation etching can be seen, due to thermal properties of the PMMA polymer; thus the LIGA process provides a higher-quality microstructure. For NaCl, the etched edges (see Fig. 2*b*) formed by the synchrotron radiation processing show no such cracks as were found in the excimer laser ablation (Küper, 1989).

4. Discussion

As we can see from Fig. 3, at least several tens of thousands of synchrotron radiation pulses are needed to etch one layer (a few Å) of the polymer, whereas a single laser pulse can ablate more than one layer (Küper, 1989). In the laser ablation (Srinivasan & Braren, 1989), there is generally a fluence *threshold* for the onset of the photo-etching (also termed 'explosive desorption') (Domen & Chuang, 1987) which proceeds layer by layer (here, the layer is not the molecular layer but is defined by Beer's law). Such a fluence threshold should not exist for the synchrotron radiation direct etching, which does not proceed layer by layer. Our measurement (Fig. 3, insert) is in agreement with this. In addition, we reduced the photon flux (used in Fig. 3) by a factor of 30 and indeed found clean pits created by the long X-irradiation with a rate of 0.13 μm min^{-1}. The fact that the synchrotron radiation etching proceeds very well may explain why we did not find any reduction in the rate, namely the transportation effect (El-Kholi *et al.*, 1994), for large aspect ratios (≫1) as well as why this process can achieve a very high aspect ratio and an

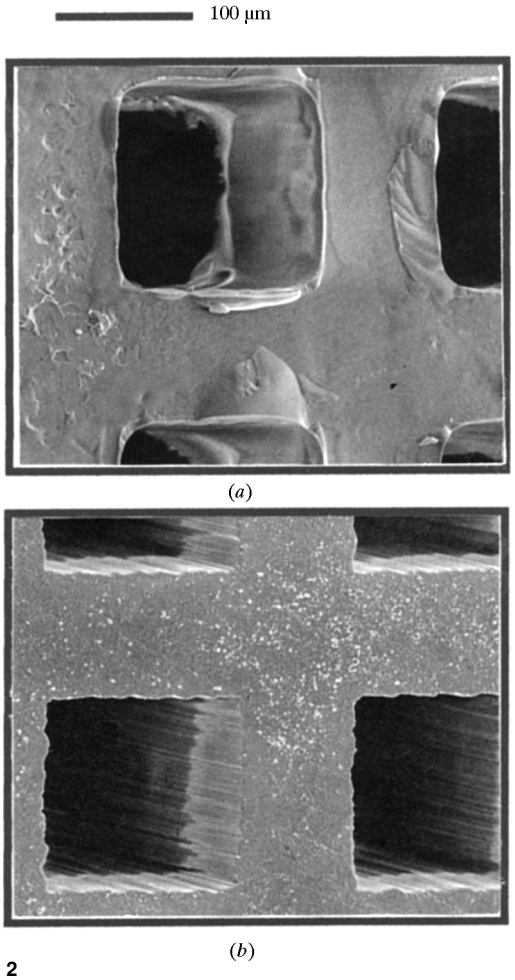

Figure 2
Scanning electron micrograph of microstructures created by synchrotron radiation direct etching in (*a*) a 200 μm-thick PMMA sheet with a structural height of 200 μm, and (*b*) a 1000 μm-thick NaCl crystal sheet with a structural height of 1000 μm.

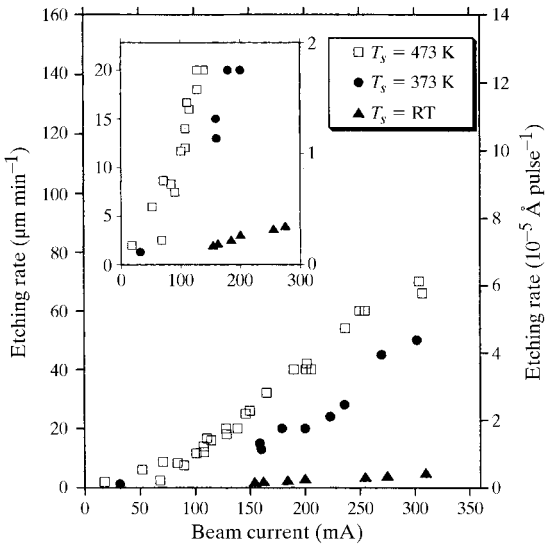

Figure 3
Etching rate (shown in two sets of units) *versus* synchrotron beam current in the case of synchrotron X-ray direct etching of PTFE at a sample temperature T_s = RT (room temperature), 373 K and 473 K. The insert shows the low-range etching-rate details more clearly.

almost zero taper angle for the etched edge. In contrast to the synchrotron radiation etching, the pulse etching rate (*e.g.* 0.1 μm pulse^{-1}) of the laser ablation is much higher and an ablation plume (a dense cloud of ablated materials) is usually generated. There are some effects induced by the ablation plume, *e.g.* the beam-size effect, where the ablation rate for a larger irradiation surface may become smaller due to shielding of the laser pulse by the plume (Eyett & Bäuerle, 1987). In contrast to this, the rate of the synchrotron radiation etching was found to become larger for a larger irradiation surface. In conclusion, the synchrotron radiation direct etching process is essentially different from the ablation induced by laser pulses and thus should not be termed 'ablation'.

In order to gain some understanding of the decomposition mechanism, an *in situ* mass spectrometric diagnosis was carried out using a quadrupole mass spectrometer to detect gaseous species evolved upon synchrotron radiation etching of PTFE (Zhang & Katoh, 1996). All mass distributions obtained were similar irrespective of whether the the substrate temperature was increased or the synchrotron radiation beam was switched from white light to X-rays, *i.e.* the predominant signal CF_3^+ was detected at 69 a.m.u., due to saturated fluorocarbons CF_3–C_nF_{2n}–CF_3 as the gaseous etching products. The synchrotron radiation dissociation of PTFE, in which the saturated fluorocarbons are the main gaseous products, is completely different from *thermal* dissociation of PTFE in which the monomers C_2F_4 are the main gaseous products. Therefore, the synchrotron radiation etching process should also not be termed 'evaporation' as in the laser-evaporation case which results from laser heating.

Based on the literature and our study, the reaction process under synchrotron irradiation with different photon flux is understood as follows.

4.1. *Under low photon flux (e.g. 10^{15} photons s^{-1} cm^{-2}) at T_s = RT*

For the polymers, absorption of the X-ray photons leads to dissociation of chemical bonds to form fragments, which may react with neighbouring fragments to form a cross-linked network or desorb from the surface if they are small enough (Simons *et al.*, 1994). This degradation (also termed 'incubation') process may result in visible discolouration and pitting of the polymer surface. For the NaCl crystal, X-irradiation at T_s = RT causes defects in the crystalline lattice, resulting in visible colour centres (Seitz, 1954) and also the desorption of atomic species (Szymonski *et al.*, 1992). We observed the colour centres at T_s = RT under the low X-photon flux, with bleaching as the substrate temperature increased.

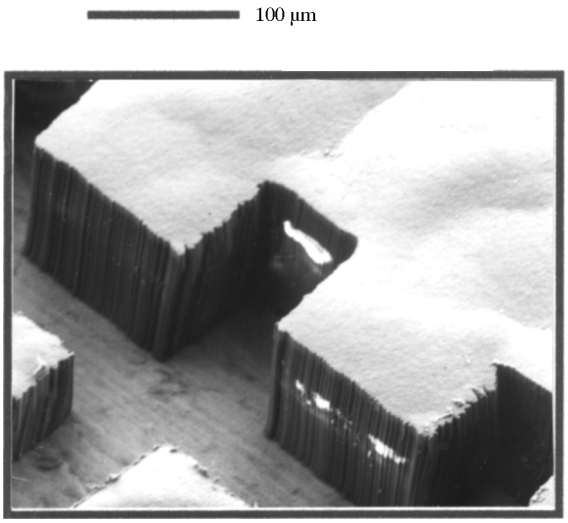

Figure 4
Scanning electron micrograph of 100 μm-thick microstructures created by Ni-electroforming in a 300 μm-thick PTFE template on a Cu substrate followed by synchrotron radiation photo-etching of the PTFE template.

4.2. *Under high photon flux (e.g. 10^{17} photons s^{-1} cm^{-2}) and increasing the substrate temperature*

Though the main dissociation mechanism may not change, the desorbing rate becomes considerably larger and the surface is etched into the bulk following patterns (defined by the mask) of the synchrotron radiation beam. This is the so-called photo-etching process which may result in the high-aspect-ratio microstructures. The explosive desorption, like the laser ablation, however, does not occur under the present synchrotron radiation conditions. In the case of PMMA, both the UV excimer laser ablation and UV photo-etching are well known, providing a good example for distinguishing the ablation from the photo-etching: ablation occurs only when a laser pulse reaches a certain fluence threshold, whereas photo-etching occurs even under continuous UV light; the laser ablates the polymer layer by layer (pulse by pulse) with a dynamic rate of 0.11 μm/20 ns (= 3.3 × 10^8 μm min^{-1}), while the UV light etches the polymer with a rate of 2 × 10^{-3} μm min^{-1} at T_s = 333 K (Ueno *et al.*, 1981). Although the etching rate for synchrotron radiation (Table 1) can be 10^4 times larger than that for UV light, the synchrotron radiation process is still essentially different from the laser ablation. Since there is no threshold for the synchrotron radiation etching process, the long X-irradiation with the low photon flux in the case of X-ray lithography can result in clean pits on the PMMA surface with the small etching rate, namely self-development (Yamada *et al.*, 1988). In our case, the self-development in PMMA was found to have a depth of 4–20 μm and a rate of 0.03–0.22 μm min^{-1}. It should be noted that the increase in the sample temperature T_s may play a considerable role in desorption to enhance the etching rate for the synchrotron radiation processing, but would not take over the role of the X-ray photons in the dissociation. The Arrhenius-like plot for the etching rate [μm (100 mA)$^{-1}$ min^{-1}] gave a slope of 0.1 eV in our case for PTFE, smaller than 0.7 eV in the case of the synchrotron radiation direct photo-etching of SiO_2 (Akazawa *et al.*, 1990), and much smaller than 3.6 eV, the activation energy for vacuum pyrolysis of PTFE (Single *et al.*, 1964). As mentioned above, mass spectrometric analysis in the case of PTFE has also provided evidence that the dissociation of PTFE during the synchrotron radiation process is completely different from thermal dissociation.

5. Outlook

The microstructures made of PTFE cannot only be microparts (see Fig. 1) but can also be used as templates for metallic electroforming when the microstructures have been formed on conducting substrates. Fig. 4 shows the nickel microstructures formed by electroforming, which was carried out in a PTFE template on a copper substrate, followed by synchrotron radiation direct etching of the PTFE template. The metallic electroforming is almost the same as that performed in the LIGA

process. We are going to carry out an LIGA-like process by replacing the hard X-ray deep lithography with the synchrotron radiation direct photo-etching. Compared with the hard X-ray deep lithography, the direct photo-etching has the following advantages: it needs no high-energy synchrotron radiation source nor high-contrast X-ray masks, but it has much higher processing rates.

References

Akazawa, H., Utsumi, Y., Takahashi, J. & Urisu, T. (1990). *Appl. Phys. Lett.* **57**, 2302–2304.

Domen, K. & Chuang, T. J. (1987). *Phys. Rev. Lett.* **59**, 1484–1487.

El-Kholi, A., Mohr, J. & Stransky, R. (1994). *Microelec. Eng.* **23**, 219–222.

Eyett, M. & Bäuerle, D. (1987). *Appl. Phys. Lett.* **51**, 2054–2055.

Guckel, H. (1996). *Rev. Sci. Instrum.* **67**, 1–5.

Katoh, T. & Zhang, Y. (1997). *Microsyst. Technol.* To be published.

Küper, S. (1989). PhD thesis, University of Göttingen, Germany.

Seitz, F. (1954). *Rev. Mod. Phys.* **26**, 7–94.

Simons, J. K., Frigo, S. P., Taylor, J. W. & Rosenberg, R. A. (1994). *J. Vac. Sci. Technol.* A**12**, 681–689.

Single, J. G., Muus, L. T., Lin, T.-P. & Larsen, H. A. (1964). *J. Polym. Sci. Part A*, **2**, 391–404.

Srinivasan, R. & Braren, B. (1989). *Chem. Rev.* **89**, 1303–1361.

Szymonski, M., Tyliszczak, T., Aebi, P. & Hitchcock, A. P. (1992). *Surf. Sci.* **271**, 287–294.

Ueno, N., Konishi, S., Tanimoto, K. & Sugita, K. (1981). *Jpn. J. Appl. Phys.* **20**, L709–L712.

Yamada, H., Hori, M., Morita, S. & Hattori, S. (1988). *J. Electrochem. Soc.* **135**, 966–970.

Zhang, Y. & Katoh, T. (1996). *Jpn. J. Appl. Phys.* **35**, L186–L188.